Research Article   **Open Access**

Spectroscopic Studies of the Binding Interactions of Phenothiazininum Dyes (Thionine Acetate, Azure A and Azure B) with Calf-thymus DNA

Mohan Kumar[1], Mahima Kaushik[1,2]*, Swati Chaudhary[2] and Shrikant Kukreti[2]*

[1]Cluster Innovation Centre, University of Delhi, Delhi

[2]Department of Chemistry, Nucleic Acids Research Laboratory, University of Delhi, Delhi

*Corresponding authors: Dr. Mahima Kaushik, Cluster Innovation Centre, University of Delhi, Delhi, India, Tel: +91-11-27666702; E-mail: mkaushik@cic.du.ac.in, kaushikmahima@yahoo.com

Shrikant Kukreti, Professor, Department of Chemistry, University of Delhi, Delhi, India, Tel: +91-11-27666726; E-mail: skukreti@chemistry.du.ac.in, kukretishrikant@yahoo.com

Abstract

The double helical structure of DNA offers various binding sites for the interaction of ligands or proteins. Interactions using minor groove, major groove, and through intercalation are the major types of binding mechanisms of DNA-ligand interactions. The lowering in the absorption intensity along with bathochromic shift is the indication of intercalation binding mode of the dye into the base pairs of the DNA. In this study, the interaction of phenothiazine dyes with calf-thymus DNA (ctDNA) in physiological buffer (pH 7.4) was studied using UV-visible, fluorescence, circular dichroism (CD), and UV-thermal denaturation spectroscopy. The binding constants were calculated at different temperatures with the help of fluorescence spectroscopy. CD signals signify that B-form of DNA might become more compact, upon binding of the dyes. Also, induced circular dichroism is observed which confirms the dye-DNA complex formation. Stabilization of DNA double helix upon binding with dyes was confirmed by the increase in T_m of ctDNA. Based on thermal melting profiles, it was found that thionine acetate is most promising in stabilizing the DNA double helix, in comparison to other two dyes. Also, binding constants calculated by fluorescence is in accordance with the thermal melting analysis. These results are indicative of the intercalation binding mode between dyes and the DNA. The binding affinity of the dyes to DNA is found to be in order as thionine acetate > azure A > azure B. Such preliminary studies facilitate our understanding about various types of DNA-ligand interactions and provide clues for designing new and more effective drugs.

Introduction

The interaction studies of small molecule with nucleic acids are much-explored research area due to their binding to the nucleic acid structures and their interface in transcription and replication processes. The interaction studies of ligands with the DNA are highly important in the area of chemotherapeutic applications. It is very well documented that anticancer drugs show their biological action through their interaction with the DNA molecule. To understand the molecular mechanism of the DNA-drug interaction and their effect on a particular disease, this spectroscopic study of the comparative analysis of various dyes had been planned and performed. Nucleic acids exhibit remarkable changes in absorbance and fluorescence properties after complex formation.

Thionine acetate (TA), azure A (AA), and azure B (AB) are phenothiazinium dyes with the identical basic phenothiazinium skeleton, with variations in the groups present at 3 and 7 positions (Figure 1).
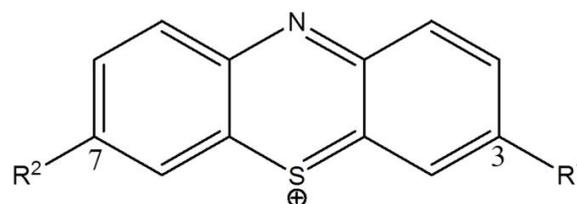
Thionine acetate: $R^1 = NH_2$, $R^2 = NH_2$
Azure A : $R^1 = NMe_2$, $R^2 = NH_2$
Azure B : $R^1 = NMe_2$, $R^2 = NHMe$

Figure 1: Chemical structure of (a) Thionine acetate, (b) Azure A, and (C) Azure B.

Thionine (3,7-diamino-5-phenothiazinium) is a planar phenothiazinium dye that consists of a heterocyclic nitrogen atom with two amine groups present at 3 and 7 positions of the aromatic ring [1]. It is widely used in electrochemical and photochemical biosensors [2,3]. It is also a good singlet oxygen generator and used in Photodynamic Therapy (PDT) [4,5]. The interaction studies of thionine acetate with the DNA molecule under various conditions

have been well reported [6,7]. It is extensively used in nucleic acid probes [1], decontamination of blood products [8], and against bacteria, viruses, and yeast [9-11]. The interaction studies of thionine with the DNA, by taking advantage of numerous biophysical techniques have already been reported and have shown that the thionine binds to DNA by two different modes, intercalation as well as outside the DNA double helix [12]. They also suggest that thionine does not show the binding affinity towards GC-rich sequences. Later, it was proposed that the thionine binding to GC-rich sequence is preferable in comparison to AT-rich sequences [13]. Brown and Brown have reported that TA has mutagenic activity against eukaryotic cells [14]. It is reported that phenothiazinium dye methylene blue (MB) has the potential to inhibit acetylcholinesterase (AChE) and butyrylcholinesterase (BuChE). The pharmacological action of MB is assisted by one of its metabolite i.e., azure B, which is able to inhibit AChE with twofold lower potency and BuChE with fivefold lower potency as compared to MB [15]. It is also documented that azure B has significance in Alzheimer's disease, where it can inhibit the formation of ß-amyloid protein filament [16]. Azure A and azure B can potentially inhibit the formation of tau filament with IC_{50} values without affecting the ability of tau protein to interact with microtubules [17]. An effective and accurate LC-MS/MS analytical method was developed by Kim and their coworkers to quantify the methylene blue and its metabolite azure B which is used in the pharmacokinetic studies of phenothiazine dyes [18].

Azure A is a cationic dye belonging to the phenothiazinium group having an asymmetrical structure. It is commonly used as a therapeutic agent due to its potential biological activity. Other biological activity of azure A dye includes anti-malarial activity [19], reducing the extent of arrhythmias [20], and diagnosis of amyloid accumulation related diseases. It is well-known staining dye, used to stain blood smear and also in electrochemical biosensing [21]. In a report, azure A is employed as an agent who is capable of detecting the anionic detergents present in milk [22].

Azure B, monodemethyl methylene blue is very close in structure to azure A, and is also biologically important dye used for staining purpose. It is widely used for staining DNA, proteins, viruses, melanin, keratin fibers, and malaria-infected cells [23]. It has also anti-inflammatory and antitumor properties [24]. This dye is used in the treatment of oral cavity infection, nail infection, Alzheimer disease, diabetes, and detection of oral cancer [25].

Although lot of interaction studies of these dyes are reported in the literature, but their comparative analysis is not discussed in detail. Here, we report the intercalation of all the three phenothiazinium dyes with calf thymus DNA using various spectroscopic studies such as circular dichroism, fluorescence spectroscopy, UV-visible absorptions spectroscopy, and UV-thermal melting studies. The basic difference between the three dyes is the presence of methyl group on the functional group which is responsible for increasing the hydrophobicity of the dye. In an attempt of the comparative analysis of binding constant values, it was found that thionine dye can interact with ct-DNA most efficiently among all the three (Thionine acetate, azure A and azure B). The quenching constants were also calculated and it was concluded that all the three dyes are interacting with DNA in the same manner, with difference in their extent of binding.

Materials and Methods

Calf thymus DNA was purchased from S.G Enterprises and used without further purification. Thionine acetate, azure A, and azure B were purchased from Helix Biosciences. The stock solution of both ctDNA and all the ligands were prepared by dissolving in double distilled water and a working solution was prepared by appropriate dilution. The concentration of ctDNA was determined by recording absorption of ctDNA at 260 nm (ε_{260}=6600 L.mol^{-1}.cm^{-1}). Sodium cacodylate (pH=7.4, containing 0.1 M NaCl and 0.1 mM EDTA) was used as buffer solution. All chemicals were of analytical grade.

UV-Vis Spectroscopic experiments

The UV-absorption spectra was recorded on a UV-1650 PC Shimadzu UV-visible spectrophotometer (TMSPC-8(E)-200) and interfaced with a Pentium IV computer for data collection and analysis. The stoppered quartz cuvette of 1 cm optical path length (1 ml volume) was used for the UV-experiments.

Thermal melting studies

UV-thermal melting experiments of ctDNA were performed at 260 nm in the absence and presence of the dyes on a UV-2450 PC Shimadzu UV-visible spectrophotometer (TMSPC-8(E)-200) and interfaced with a Pentium IV computer for data collection and analysis. The temperature gradient used was 20-95°C at a rate of 0.5°C/min. The T_m values of ctDNA and their complex were obtained from the midpoint of the transition of melting curves.

Fluorescence measurements

The fluorescence spectra and intensity were recorded on Cary Eclipse spectrofluorimeter (Varian, USA) equipped with a 150W Xenon lamp with a 1 cm quartz cuvette and a thermostat water bath. The pH was measured on a Thermo scientific Orion 2 star pH meter (Singapore). Fluorescence spectra of all the three drugs were obtained at 290 K, 300 K, and 310 K temperature in the range 590-800 nm at an excitation wavelength 595, 625, and 640 nm for TA, AA, and AB respectively, using a slit width of 5 nm.

Circular Dichroism (CD) studies

The CD spectra were recorded on JASCO J-815 spectropolarimeter using a quartz cuvette of 1.0 cm path length, at wavelength 200-700 nm, 1 nm data pitch with a response time of 1 s and averaged of accumulation of three scans at a speed of 100 nm/min.

Result and Discussion

UV absorption studies

Absorption studies are considered the most common and elementary technique to explore the interaction studies of dyes with the DNA by observing the changes in the absorption spectrum of either DNA or drug molecule [26,27]. Usually, interaction studies are carried out by varying the concentration of calf thymus DNA with a fixed concentration of ligand/proteins. The visible absorption spectra show maxima at 598 nm, 631 nm, 646 nm for thionine acetate, azure A, and azure B respectively. A small hump can also be noticed at 561 nm, 588 nm, and 598 nm for all the three dyes. Figure 2 shows UV-absorption spectra of all the three dyes on increasing concentrations of

calf thymus DNA. As the concentration of calf thymus DNA is increased, the absorbance starts decreasing, resulting in hypochromic effect. Apart from this, a bathochromic shift of 7 nm from 631 nm to 638 nm and of 4 nm from 646 nm to 650 nm in maximum absorption peaks of azure A and azure B dyes are observed respectively. While in the case of thionine acetate, a red shift of 6 nm in the absorption maxima from 598 nm to 604 nm is detected. The absorption intensity decreases along with bathochromic shift in the case of intercalation binding mode of the dyes into the base pairs of the DNA [28]. The dye molecule intercalates via coupling of empty π^* orbital of the dye molecule with the π^* orbital of the DNA base pairs. As a result, π- π^* electronic energy decreases which leads to red shift. The hypochromic effect is caused due to the reduced probability of transition because of partially filled empty π^* orbital. Sharp isosbestic points at 652 nm, 660 nm, and 611 nm observed for azure A, azure C and thionine acetate respectively, confirming the existence of an equilibrium between the two states of free and bound dye molecules. These results indicate towards the presence of intercalation mode of binding between dyes and the DNA double helix.

Fluorescence spectroscopic experiments

Fluorescence spectroscopy is extensively used to explore the binding mechanism of a ligand to the protein or DNA molecule [29]. An external molecule can potentially quench the fluorescence of any molecule upon binding. Several types of molecular interactions are liable for the quenching of the fluorescence, including complex formation in the ground state, excited-state reactions, molecular rearrangements, energy transfer, and collisional quenching [30]. The fluorescence emission spectra of thionine acetate, azure A, and azure B in the absence and presence of DNA are displayed in Figure 3. Thionine acetate, azure A, and azure B are fluorescent molecules: when excited at 595, 625, and 640 nm, the emission spectra in the range of 600-700 nm with maxima at 623, 653, and 672 nm respectively is observed. Keeping the constant concentration of dye, the DNA concentration was gradually increased, in order to examine the complex formation. The quenching in the fluorescence spectrum is observed with all the three dyes, on each addition of DNA, suggesting the confirmation of the complex formation. The maximum quenching (~69%) in the fluorescence was detected for TA-DNA complex, followed by azure A (~55%) and the least for azure C (~69%). A similar pattern for quenching is already reported; where it is shown

that the quenching of azure A is much prominent in comparison to azure B [31]. The obtained fluorescence quenching is the consequence of the successful binding of the dye molecule to the base pairs of DNA.

Fluorescence intensities of dye samples were rectified for the respective absorbance of dyes at emission and excitation wavelengths of the fluorescence data. Corrections for the inner filter effect were implemented using the following equation [32].

The Binding parameters

The fluorescence quenching due to binding of the dye to ctDNA was further utilized to calculate the binding efficiency (K_b). The binding constant (K_b) at various temperature can be attained by using the following equation [33,34].

Values of K_b were determined by the intercept of the plot of log [(F_0-F)/ F] versus log [Q] (Figure 3). The binding constants for all the three dyes are calculated and shown in Table 1.

Thionine Acetate			
S. No.	T(K)	K_b (Lmol^{-1})	K_{SV} (Lmol^{-1})
1	290	6.88 × 106	1.73 × 105
2	300	4.5 × 106	1.3 × 105
3	310	5.11 × 105	1.03 × 105
Azure A			
1	290	5.95 × 105	6.13 × 104
2	300	3.47 × 105	5.5 × 104
3	310	1.06 × 105	4.57 × 104
Azure B			
1	290	1.03 × 105	7.37 × 104
2	300	4.0 × 104	5.3 × 104
3	310	6.3 × 103	7.0 × 103

Table 1: Binding constant and quenching constant values calculated from fluorescence spectra.
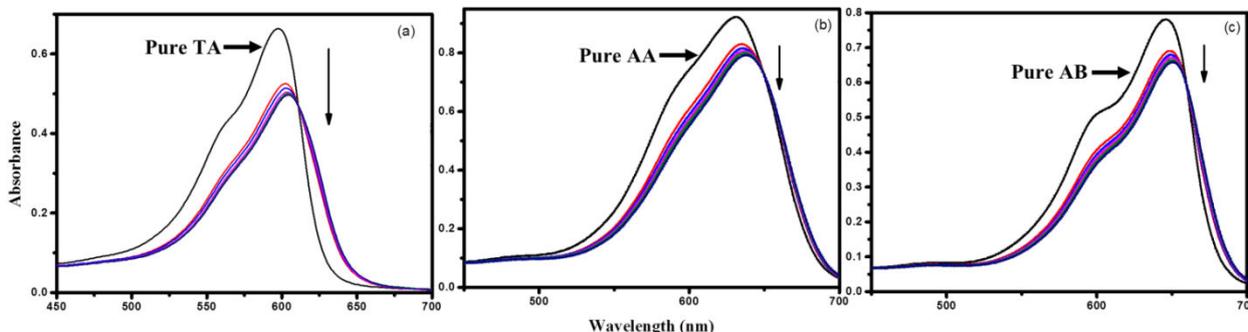

Figure 2: UV absorption spectra of Thionine acetate (a), Azure A (b), and Azure B (c) varying with concentrations of ctDNA at pH=7.4 and T=300 K, C_{Dye}=0 µmol.L^{-1}, C_{DNA}=0, 100, 120, 140, 160, and 180 µmol.L^{-1} for curves 1-8, respectively.
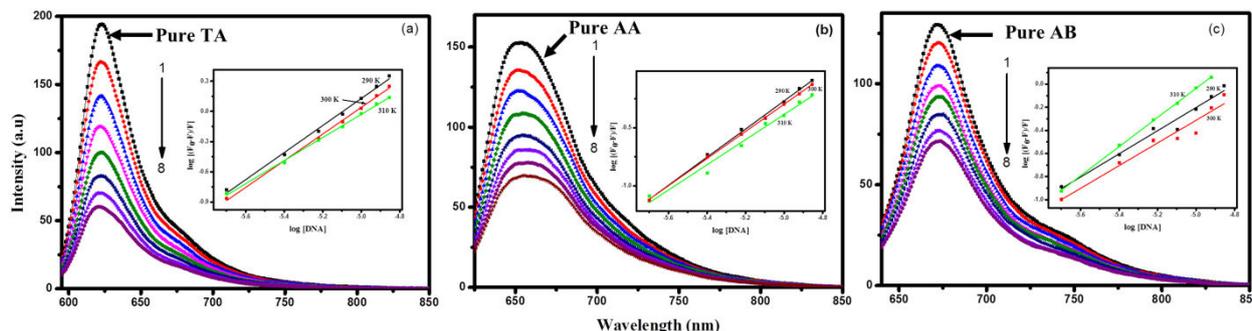
Figure 3: (a) Fluorescence spectra of (a) TA, (b) AA, and (c) AB in the presence of ctDNA at different concentrations at pH=7.4 and T=300 K, C_{Dye}=10 μmol.L^{-1}, C_{DNA}=0, 20, 40, 60, 80, 100, 120, and 140 μmol.L^{-1} for curves 1-8, respectively (Inset: The plot of log $(F_0-F)/F$ versus log [DNA]).

The quenching mechanism

It has been noticed that the fluorescence emission intensity of the dyes is gradually decreased with the increase in the concentration of ctDNA. It means that ctDNA could quench the intrinsic fluorescence of the dyes. The fluorescence quenching constant at different temperatures (290 K, 300 K, and 310 K) was calculated using the Stern-Volmer equation (Figure 4) [35].
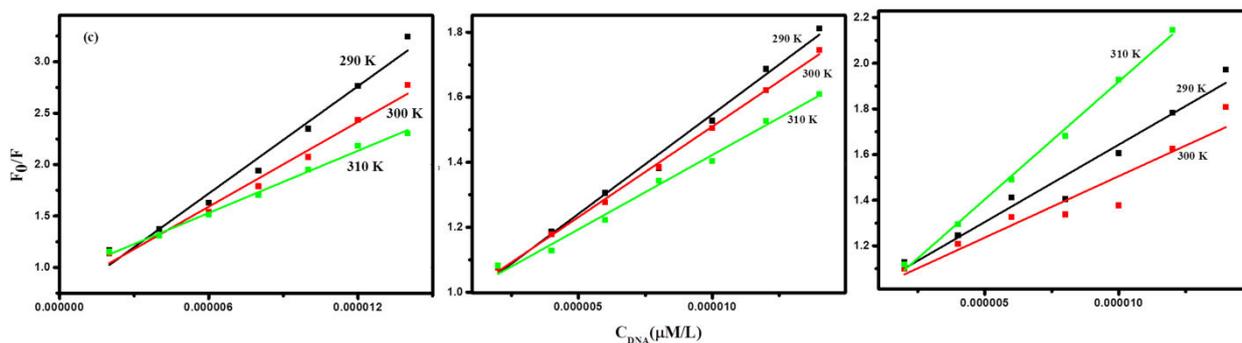

Figure 4: Stern-volmer plots for the quenching of (a) TA, (b) AA, and (c) AB by DNA at different temperatures.

Where F_0 and F are the fluorescence intensities of the dyes in the absence and presence of the quencher, respectively, [Q] is the concentration of the quencher and K_{SV} is the Stern-Volmer quenching constant, which can be determined by the plot of F_0/F against [Q]. The different types of quenching are generally categorized as either static or dynamic quenching. The static and dynamic quenching constants are totally temperature dependent. The K_{SV} values signify the fluorophore accessibility to the quencher. It was concluded that quenching constant (K_{SV}) decreases with the increase in temperature, which signifies the presence of static quenching between the dyes and ctDNA [36].

Circular dichroism

Circular Dichroism (CD) is a very sensitive and accurate technique to study the optical behavior of any chiral molecule. It gives the information of the secondary structure of nucleic acid and proteins. It can easily discriminate between various secondary structures formed by DNA (A-, B-, Z- etc.) [37]. All the forms of DNA have a unique CD spectrum with different wavelength maxima and the ellipticity. The B-form of the DNA is comprised of a positive peak around 270-280 nm, due to base stacking and a negative peak at 245 nm, due to right-handed helicity [38]. The conformational changes in the secondary structure of ctDNA have been studied using circular dichroism spectroscopy. The CD spectrum in the range of 200-320 nm was examined to see the effect of dye-induced changes in the DNA secondary structure in the presence of various concentrations of the dyes. Circular dichroism spectra of ctDNA (1×10^{-4} M) was recorded in the presence of increasing amounts of dye at the following stoichiometric ratios: r_i=[dye]/[DNA]=0.0, 0.10, 0.15 in the wavelength range 200-320 nm, at 298 K temperature (Figure 5).
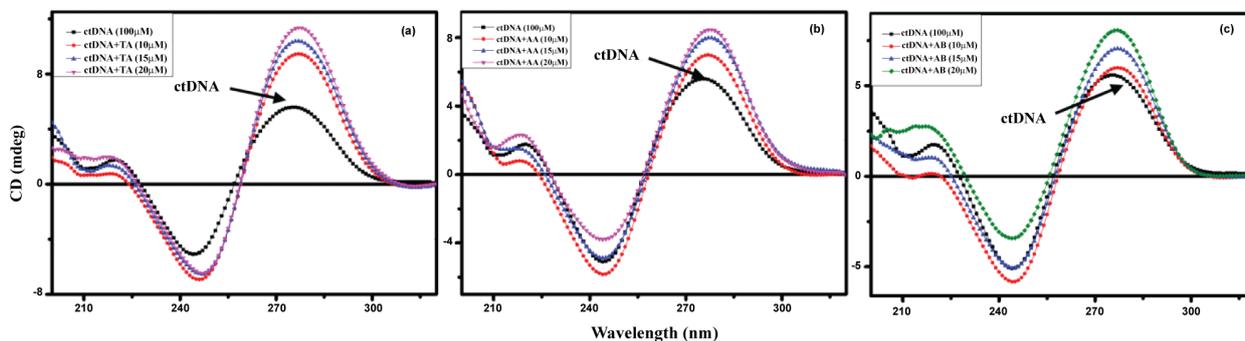
Figure 5: Circular Dichroism spectra of DNA(1×10^{-4} M) in sodium cacodylate buffer (20 mM, pH 7.4) in the presence of increasing amounts of dyes (a) TA, (b) AA, and (c) AB at the following stoichiometric ratios: r_i=[dye]/[DNA]=0.0, 0.1, 0.15, 0.2.

The CD spectrum of ctDNA consisted of a positive peak at 275 nm and a negative peak at 244 nm, which is characteristic of B-form of DNA. An increase in the positive peak at 275 nm is observed on addition of dye to it, which is in turn result of intercalation of dye into the DNA base pairs [39]. An increment in the intensity at 245 nm has also been noticed, giving an indication of stabilization in the right-handed more compact B-form of DNA [40]. All the dyes used in this study (TA, AA, and AB) as well as ctDNA do not show optical behavior around 400 to 700 nm range individually, while their complexes (DNA-dyes) have shown optical active nature, which is attributed to induced circular dichroism [41,42]. Figure 6 depicts the induced circular Dichroism spectral changes of TA, AA and, AB upon binding to ctDNA which quite clearly confirms the the formation of the DNA-dye complex in all cases.
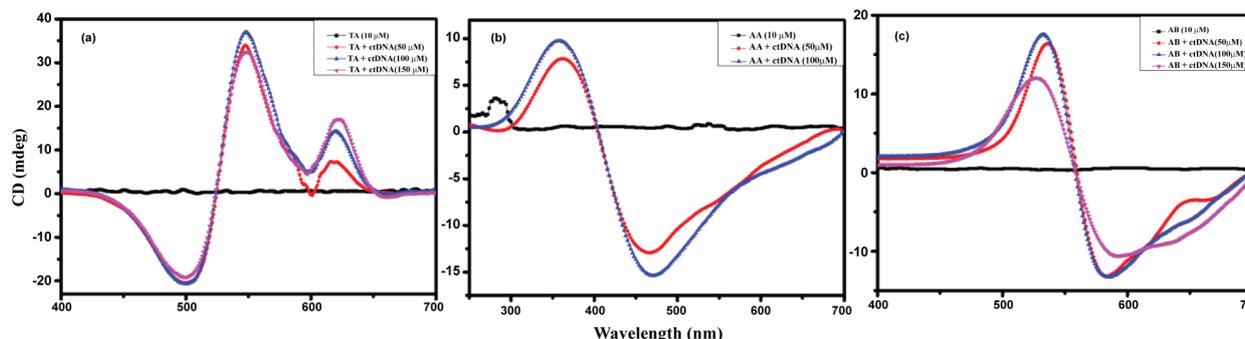

Figure 6: Circular Dichroism spectra of Dyes (10 μM) (a) TA, (b) AA, and (c) AB in sodium cacodylate buffer (20 mM, pH 7.4) in the presence of increasing amounts of DNA.

Thermal-denaturation studies

The thermal stability of DNA can be determined by employing UV-thermal denaturation technique. The absorbance increases sigmoidally, when DNA sample is heated and the temperature at which half of the DNA gets unwind is known as the melting temperature (Tm). It helps in the detection of stabilization or destabilization of a DNA structure on interaction with a ligand [43,44]. Experimental evidences suggest that intercalative mode of binding is attributed to increase in T_M value up to 3-8°C, whereas no significant change is observed in T_M value for non-intercalative interaction [45]. Figure 7 represents the melting curves of calf thymus DNA at 260 nm in the absence or presence of dyes. A melting temperature of 84°C was observed for calf thymus DNA in the absence of dyes under physiological conditions [46], however the melting temperature in the presence of thionine acetate, azure A, and azure B were found to be 89°C, 86.5°C, and 86°C respectively. As can be seen from the results, the interaction with all the three dyes causes a significant increase in the denaturation temperature, which strongly recommends the intercalation mode of

binding of dyes. The binding constant calculated by the fluorescence spectroscopy manifested that the TA could bind to DNA more efficiently in comparison to other two dyes. A similar pattern is observed from the thermal melting profiles as well. The melting temperature of TA-DNA complex was found to 4°C more than the alone DNA melting temperature, while in the case of AA and AB, it was found only around 1°C or 2°C. The thermal melting analysis is also in accordance with the fluorescence data.

Conclusion

In the present work, the spectroscopic analysis of the interaction of the three phenothiazinium dyes (Thionine acetate, azure A, Azure B) with ctDNA was carried out using biophysical techniques such as UV-absorption, fluorescence, circular dichroism and thermal melting analysis. In UV-spectra of the dyes, a hypochromic and red shift was detected with the increasing concentrations of ctDNA, suggesting the intercalation mode of binding. The binding constant and quenching

constant was calculated using fluorescence spectroscopy. The K_b value decreases with the rise in temperature, due to a decrease in the association between the dyes and ctDNA. CD results indicated the stabilization of B-form of DNA on dye binding. An increase in the melting temperature in case of all the three dyes indicates the intercalation binding mode. Thionine acetate had shown the maximum DNA stabilization the DNA double helix among all the studied dyes. The order in which these dyes stabilize the DNA double helix is TA > AA > AB, which was confirmed by the binding constants value and their melting profiles. All the results presented here are indicative of intercalation mode of binding between the dyes and ctDNA. This report provides insights on the interaction of ligands with DNA and adds to the knowledge towards findings of more efficient molecules for DNA binding.
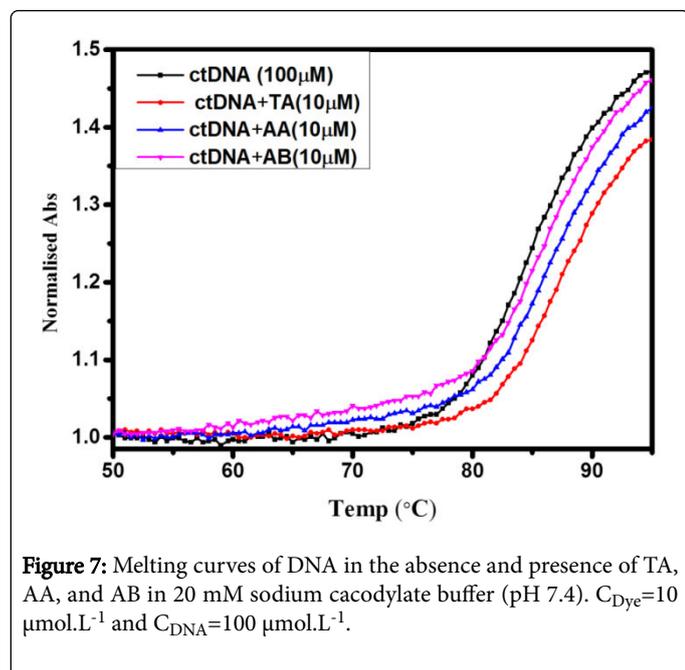

Figure 7: Melting curves of DNA in the absence and presence of TA, AA, and AB in 20 mM sodium cacodylate buffer (pH 7.4). C_{Dye}=10 $\mu mol.L^{-1}$ and C_{DNA}=100 $\mu mol.L^{-1}$.

Acknowledgments

References

1. Tuite EM, Kelly JM (1993) New trends in photobiology: photochemical interactions of methylene blue and analogues with DNA and other biological substrates. J Photochem Photobiol B Biol 21: 103-124.

2. Xu Y, Yang L, Ye X, He P, Fang Y (2006) Impedance-Based DNA Biosensor Employing Molecular Beacon DNA as Probe and Thionine as Charge Neutralizer. Electroanalysis 18: 873-881.

3. Deng L, Wang Y, Shang L, Wen D, Wang F, et al. (2008) A sensitive NADH and glucose biosensor tuned by visible light based on thionine bridged carbon nanotubes and gold nanoparticles multilayer. Biosens Bioelectron 24: 951-957.

4. Tardivo JP, Del Giglio A, de Oliveira CS, Gabrielli DS, Junqueira HC, et al. (2005) Methylene blue in photodynamic therapy: from basic mechanisms to clinical applications. Photodiagnosis Photodyn Ther 2: 175-191.

5. Gabrielli D, Belisle E, Severino D, Kowaltowski AJ, Baptista MS (2004) Binding, aggregation and photochemical properties of methylene blue in mitochondrial suspensions. Photochem Photobiol 79: 227-232.

6. Paul P, Hossain M, Yadav RC, Kumar GS (2010) Biophysical studies on the base specificity and energetics of the DNA interaction of photoactive dye thionine: spectroscopic and calorimetric approach. Biophys Chem 148: 93-103.

7. Baranovskii SF, Bolotin PA, Evstigneev MP, Chernyshev DN (2008) Complexation of heterocyclic ligands with DNA in aqueous solution. J Appl Spectrosc 75: 251-260.

8. Svoboda V, Cooney MJ, Rippolz C, Liaw BY (2007) In situ characterization of electrochemical polymerization of methylene green on platinum electrodes. J Electrochem Soc 154: 113-116.

9. Wainwright M (2005) The development of phenothiazinium photosensitisers. Photodiagnosis Photodyn Ther 2: 263-272.

10. Phoenix DA, Sayed Z, Hussain S, Harris F, Wainwright M (2003) The phototoxicity of phenothiazinium derivatives against Escherichia coli and Staphylococcus aureus. FEMS Immunol Med Microbiol 39: 17-22.

11. Wainwright M (1988) Photodynamic antimicrobial chemotherapy (PACT). J Antimicrob Chemother 42: 13-28.

12. Tuite E, Kelly JM (1995) The interaction of methylene blue, azure B, and thionine with DNA: formation of complexes with polynucleotides and mononucleotides as model systems. Biopolymers 35: 419-433.

13. Paul P, Kumar GS (2010) Toxic interaction of thionine to deoxyribonucleic acids: Elucidation of the sequence specificity of binding with polynucleotides. J Hazard Mater 184: 620-626.

14. Brown JP, Brown RJ (1976) Mutagenesis by 9, 10-anthraquinone derivatives and related compounds in Salmonella typhimurium. Mutat Res Genet Toxicol 40: 203-224.

15. Petzer A, Harvey BH, Petzer JP (2014) The interactions of azure B, a metabolite of methylene blue, with acetylcholinesterase and butyrylcholinesterase. Toxicol Appl Pharmacol 274: 488-493.

16. Taniguchi S, Suzuki N, Masuda M, Hisanaga SI, Iwatsubo T, et al. (2005) Inhibition of heparin-induced tau filament formation by phenothiazines, polyphenols, and porphyrins. J Biol Chem 280: 7614-7623.

17. Oz M, Lorke DE, Petroianu GA (2009) Methylene blue and Alzheimer's disease. Biochem Pharmacol 78: 927-932.

18. Kim SJ, Ha DJ, Koo TS (2014) Simultaneous quantification of methylene blue and its major metabolite, azure B, in plasma by LC-MS/MS and its application for a pharmacokinetic study. Biomed Chromatogr 28: 518-524.

19. Vennerstrom JL, Makler MT, Angerhofer CK, Williams JA (1995) Antimalarial dyes revisited: xanthenes, azines, oxazines, and thiazines. Antimicrob Agents Chemother 39: 2671-2677.

20. Paul P, Kumar GS (2013) Spectroscopic studies on the binding interaction of phenothiazinium dyes toluidine blue O, azure A and azure B to DNA. Spectrochim Acta Mol Biomol Spectrosc 107: 303-310.

21. Yao H, Li N, Xu S, Xu JZ, Zhu JJ, et al. (2005) Electrochemical study of a new methylene blue/silicon oxide nanocomposition mediator and its application for stable biosensor of hydrogen peroxide. Biosens Bioelectron 21: 372-377.

22. Barui AK, Sharma R, Rajput YS (2012) Detection of non-dairy fat in milk based on quantitative assay of anionic detergent using azure A dye. Int Dairy J 24: 44-47.

23. Khan AY, Kumar GS (2016) Spectroscopic studies on the binding interaction of phenothiazinium dyes, azure A and azure B to double stranded RNA polynucleotides. Spectrochim Acta Mol Biomol Spectrosc 152: 417-425.

24. Čulo F, Sabolović D, Somogyi L, Marušić M, Berbiguier N, et al. (1991) Anti-tumoral and anti-inflammatory effects of biological stains. Agents Actions 34: 424-428.

25. Wischik CM, Edwards PC, Lai RY, Roth M, Harrington CR (1996) Selective inhibition of Alzheimer disease-like tau aggregation by phenothiazines. Proc Natl Acad Sci 93: 11213-11218.

26. Sirajuddin M, Ali S, Badshah A (2013) Drug–DNA interactions and their study by UV–Visible, fluorescence spectroscopies and cyclic voltametry. J Photochem Photobiol B Biol 124: 1-19.

27. Agarwal S, Jangir DK, Mehrotra R (2013) Spectroscopic studies of the effects of anticancer drug mitoxantrone interaction with calf-thymus DNA. J Photochem Photobiol B Biol 120: 177-182.

28. Iyengar G, Ashrit R, Ashish A, Sharma K, Gupta MD, et al. (2014) Elucidation of drug–DNA intercalation binding mode. Curr Sci 107: 954.

29. Sridharan R, Zuber J, Connelly SM, Mathew E, Dumont ME (2014) Fluorescent approaches for understanding interactions of ligands with G protein coupled receptors. BBA Biomemb 1838: 15-33.

30. Hu T, Liu Y (2015) Probing the interaction of cefodizime with human serum albumin using multi-spectroscopic and molecular docking techniques. J Pharm Biomed Anal 107: 325-332.

31. Wang Q, Liu X, Su M, Shi Z, Sun H (2015) Study on the interaction characteristics of cefamandole with bovine serum albumin by spectroscopic technique. Spectrochim Acta Mol Biomol Spectrosc 136: 321-326.

32. Santos-Carballal B, Swamy MJ, Moerschsbacher BM, Goycoolea FM (2016) SYBR Gold fluorescence quenching is a sensitive probe of chitosan-microRNA interactions. J Fluoresc 26: 37-42.

33. Alam P, Chaturvedi SK, Anwar T, Siddiqi MK, Ajmal MR, et al. (2015) Biophysical and molecular docking insight into the interaction of cytosine β-D arabinofuranoside with human serum albumin. J Lumin 164: 123-130.

34. Bian W, Zhang H, Yu Q, Shi M, Shuang S, et al. (2016) Detection of Ag^+ using graphite carbon nitride nanosheets based on fluorescence quenching. Spectrochim Acta Mol Biomol Spectrosc 169: 122-127.

35. Zhang G, Hu X, Fu P (2012) Spectroscopic studies on the interaction between carbaryl and calf thymus DNA with the use of ethidium bromide as a fluorescence probe. J Photochem Photobiol B Biol 108: 53-61.

36. Ajloo D, Shabanpanah S, Shafaatian B, Ghadamgahi M, Alipour Y, et al. (2015) Interaction of three new tetradentates Schiff bases containing N_2O_2 donor atoms with calf thymus DNA. Int J Biol Macromolec 77: 193-202.

37. Jiang S, Liu HZ, Cai WL, Bai AM, Ouyang Y, et al. (2016) Quasi-spherical silver nanoparticles with high dispersity and uniform sizes: preparation, characterization and bioactivity in their interaction with bovine serum albumin. Luminescence 31: 1146-1151.

38. Chang YM, Chen CKM, Hou MH (2012) Conformational changes in DNA upon ligand binding monitored by circular dichroism. Int J Mol Sci 13: 3394-3413.

39. Awasthi P, Kumar N, Kaushal R, Kumar M, Kukreti S (2015) Comparative In Vitro Binding Studies of TiCl2 (dpme) 2, Ti (ada) 2 (bzac) 2, and TiCl2 (bzac)(bpme) Titanium Complexes with Calf-Thymus DNA. Biochem Res Int 2015.

40. Berdnikova DV, Ihmels H, Schönherr H, Steuber M, Wesner D (2015) Photoinduced formation of stable Ag-nanoparticles from a ternary ligand-DNA-Ag^+ complex. Org Biomol Chem 13: 3766-3770.

41. Zhong W, Yu JS, Liang Y, Fan K, Lai L (2004) Chlorobenzylidine–calf thymus DNA interaction II: circular dichroism and nuclear magnetic resonance studies. Spectrochim Acta Mol Biomol Spectrosc 60: 2985-2992.

42. Shahabadi N, Mohammadi S (2012) Synthesis Characterization and DNA Interaction Studies of a New Zn (II) Complex Containing Different Dinitrogen Aromatic Ligands. Bioinorg Chem Appl 2012: 1-8.

43. Mergny JL, Lacroix L (2003) Analysis of thermal melting curves. Oligonucleotides 13: 515-537.

44. Kaushik M, Kaushik S, Kukreti S (2015) Exploring the characterization tools of Guanine-Quadruplexes. Front Biosci (Landmark Ed) 21: 468-478.

45. Khare D, Pande R (2012) Experimental and molecular docking study on DNA binding interaction of N-phenylbenzohydroxamic acid. Der Pharma Chem 4: 66-75.

46. Zhu J, Chen L, Dong Y, Li J, Liu X (2014) Spectroscopic and molecular modeling methods to investigate the interaction between 5-hydroxymethyl-2-furfural and calf thymus DNA using ethidium bromide as a probe. Spectrochim Acta Mol Biomol Spectrosc 124: 78-83.